

Controlling filamentation in broad-area semiconductor lasers and amplifiers

John R. Marciante^{a)} and Govind P. Agrawal

The Institute of Optics, University of Rochester, Rochester, New York 14627

(Received 20 December 1995; accepted for publication 18 May 1996)

We show that with the introduction of a new pair of epitaxial layers, sandwiched between the active and cladding regions, self-defocusing can play an important role in stabilizing the lateral mode in broad-area semiconductor lasers and amplifiers. Under certain conditions, it can be used to eliminate filamentation and provide a nearly flat mode profile by adjusting the band gap of the new self-defocusing layers. We discuss the use of a strained multiple-quantum-well laser for producing such a stable lateral mode. © 1996 American Institute of Physics. [S0003-6951(96)00331-2]

Broad-area semiconductor lasers and amplifiers are known to exhibit lateral mode instabilities, resulting in the filamentation of the near field, when the stripe width over which the current is injected exceeds 15–20 μm .^{1–6} Although thermal heating may contribute to some extent, the fundamental intrinsic nonlinear mechanism responsible for filamentation is the carrier-induced index change occurring as a result of gain saturation and the associated phenomenon of spatial hole burning. Narrow-stripe semiconductor lasers have been developed to avoid the filamentation problem. However, the filamentation issue has resurfaced again in the context of high-power master oscillator/power amplifier (MOPA) devices^{7,8} in which the output of a narrow-stripe master oscillator is amplified in a broad-area or tapered-stripe amplifier to provide high cw output powers ($\sim 2\text{--}3\text{ W}$) over a lateral region 200–300 μm wide.

In this letter we show that with the introduction of a new pair of epitaxial layers, the resonantly enhanced self-defocusing nonlinearity can play an important role in maintaining lateral-mode stability in broad-area semiconductor lasers and amplifiers. Even though these new layers are transparent to the intracavity radiation due to their larger band gap energy, a large fraction (80%–99%) of the lateral mode resides in them and experiences a nonlinear index change resulting from the third-order susceptibility. The index change Δn is quantified as $\Delta n = n_2 I$, where I is the mode intensity and n_2 is a material constant often referred to as the Kerr coefficient. If this new pair of epitaxial layers is inserted around the active region such that their band gap is larger but close to the photon energy at the lasing wavelength, then n_2 can be resonantly enhanced. Its numerical value for semiconductor lasers operating near 810 nm is measured to be $-4 \times 10^{-12}\text{ cm}^2/\text{W}$ (see Ref. 9) and higher values are possible through resonant enhancement.¹⁰

The negative values of n_2 lead to self-defocusing of the lateral mode residing in these new layers. Such self-defocusing can counteract the carrier-induced focusing of the lateral mode inside the active region and stabilize the lateral mode. Indeed, our numerical simulations show that it may be possible to design broad-area semiconductor lasers that op-

erate stably without filamentation for stripe widths as large as 100 μm .

To demonstrate the beneficial effects of the self-defocusing layers as simply as possible, we consider a broad-area semiconductor laser, operating continuously at a constant current density, and solve the intracavity forward and backward propagating waves iteratively while including diffraction, carrier diffusion, spatial hole burning, and self-defocusing. Since we are looking to solve for the lateral distribution (along the x axis) of the intracavity field, we decompose the electric field in terms of counterpropagating waves using Maxwell's equations and obtain a set of two coupled paraxial wave equations

$$\pm \frac{\partial E_m}{\partial z} = \frac{i}{2k} \frac{\partial^2 E_m}{\partial x^2} + \left[\frac{1}{2} \Gamma (1 - i\alpha) g(N) - \frac{\alpha_{\text{int}}}{2} + i(1 - \Gamma) n_2 k_0 (|E_m|^2 + 2|E_n|^2) \right] E_m, \quad (1)$$

where the + or – sign is chosen for the forward ($m=f$, $n=b$) and backward ($m=b$, $n=f$) traveling waves, respectively; $k = n_{\text{eff}} k_0$ is the mode propagation constant with n_{eff} being the effective index of refraction and $k_0 = 2\pi/\lambda$ being the free-space propagation constant. Γ is the transverse confinement factor, α is the linewidth-enhancement factor, α_{int} is internal loss, n_2 is the Kerr coefficient of the self-defocusing-layer material, and $g(N)$ is the local carrier-dependent gain assumed to be of the form $g(N) = a(N - N_0)$. Here, a is the gain cross section and N_0 is the transparency value for the carrier density ($g=0$ at $N=N_0$). The carrier density distribution can be accounted for by solving the diffusion equation¹¹

$$D \frac{\partial^2 N}{\partial x^2} = - \frac{J(x)}{qd} + \frac{N}{\tau_{\text{nr}}} + BN^2 + \frac{\Gamma g(N)}{\hbar \omega} (|E_f|^2 + |E_b|^2), \quad (2)$$

where D is the diffusion constant, $J(x)$ is the injected current density, q is the magnitude of the electron charge, d is the active-layer thickness, τ_{nr} is the nonradiative lifetime, and B is the spontaneous-emission coefficient. For uniform injection over the stripe width w , $J(x) = J_0$ for $|x| < w/2$, and 0 otherwise.

To investigate the role of the self-focusing nonlinearity, we have solved Eqs. (1) and (2) numerically by using a split-

^{a)}Also with the Semiconductor Laser Branch, USAF Phillips Laboratory, Kirtland AFB NM 87117-5776.
Electronic mail: marciant@optics.rochester.edu

step Fourier or beam-propagation method iteratively.^{11,12} The iteration procedure is initialized by assuming a super-Gaussian profile for the lateral mode. The lateral-mode profile changes initially during multiple round trips inside the laser cavity and settles down to a fixed shape after 15–20 round trips if a stable lateral mode exists for a given set of operating parameters. If the lateral mode does not stabilize even after 100 round trips and exhibits filamentary structure, the laser is quantified as “unstable” for that set of operating parameters. For our numerical simulations, we use $L=250\ \mu\text{m}$, $d=200\ \text{nm}$, $\Gamma=0.2$, facet reflectivities $R_0=R_L=0.35$, $\lambda=820\ \text{nm}$, $n_{\text{eff}}=3.5$, $\alpha_{\text{int}}=10\ \text{cm}^{-1}$, $a=1.5\times 10^{-16}\ \text{cm}^2$, $D=33\ \text{cm}^2/\text{s}$, $N_0=1.0\times 10^{18}\ \text{cm}^{-3}$, $\tau_{\text{nr}}=5\ \text{ns}$, and $B=1.4\times 10^{-10}\ \text{cm}^3/\text{s}$.

Before considering the effects of the self-defocusing nonlinearity, it is useful to consider the role of the linewidth-enhancement factor alone. As the local intensity increases, the gain saturates (spatial hole burning), thereby increasing the term $-i\alpha g(N)$ in Eq. (1), resulting in a self-focusing effect. For narrow current stripe widths, the gain is localized spatially, thus limiting detrimental effects of this focusing. However, for wide stripes this carrier-induced self-focusing can be catastrophic, leading to filamentation. This effect is combatted by diffraction, which spreads out the “hot spots” in the lateral field, and by gain saturation, which reduces the local gain, thereby allowing the surrounding regions to increase in intensity. For certain conditions, these factors can remove filamentation for small enough values of α ($\alpha<0.5$).¹³ However, since semiconductor lasers typically have α values in the range 2–6, they cannot operate stably for stripe widths in excess of $15\ \mu\text{m}$. This α -induced instability manifests as filamentation in broad-area semiconductor lasers.

As discussed earlier, the n_2 term in Eq. (1) arising from self-defocusing-layer nonlinearity has the potential of decreasing the deleterious effects of α , thereby making it possible to realize stable broad-area semiconductor lasers. For a given stripe width w and a given pumping level $r=J_0/J_{\text{th}}$, we vary n_2 over the range $-1-10\times 10^{-12}\ \text{cm}^2/\text{W}$ (since such values can be realized in practice) and find the critical boundary values of α beyond which the lateral mode destabilizes. The results are plotted in the n_2 - α plane after slight averaging to remove the numerical noise associated with finite step sizes. Figure 1 shows the stability region at two different pumping levels ($r=2.5$ and 5) for a stripe width of $50\ \mu\text{m}$. For $r=2.5$, the main effect of the self-focusing nonlinearity is to increase the critical value of α from 0.5 to above 2 for $(1-\Gamma)|n_2|>8\times 10^{-12}\ \text{cm}^2/\text{W}$. At higher pumping levels ($r=5$), the critical value of α can exceed 2 for $(1-\Gamma)|n_2|>5\times 10^{-12}\ \text{cm}^2/\text{W}$. However, a new qualitative feature appears showing that for large values of $|n_2|$, the lateral mode can become unstable even for small values of α . This can be understood by noting that α -induced and n_2 -induced changes in the mode index are of opposite sign, and the two must be balanced for realizing stable operation of broad-area semiconductor lasers.

To underscore the mode quality, Figs. 2(a) and 2(b) show the near-field and far-field profiles, respectively, for laser operation at 2.5 times above threshold when $\alpha=1$, and $(1-\Gamma)n_2=-5\times 10^{-12}\ \text{cm}^2/\text{W}$. For $n_2=0$, the numerically

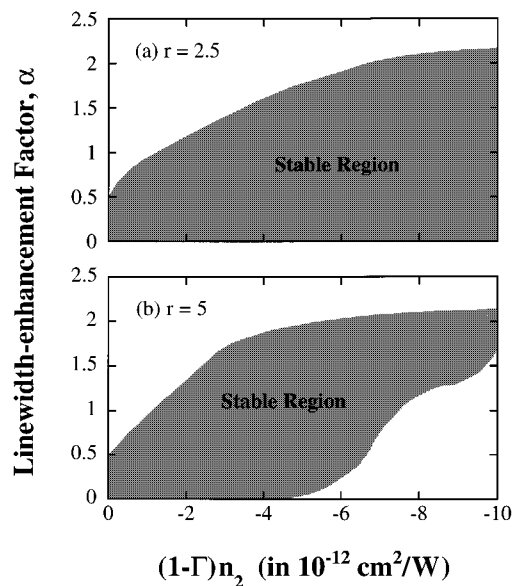


FIG. 1. Stable operation regions in the n_2 - α plane for a $50\text{-}\mu\text{m}$ -stripe-width laser operating (a) 2.5 times above threshold and (b) 5 times above threshold. The boundaries of these regions mark the values of α for which the lateral mode becomes unstable at a given value of n_2 .

simulated mode exhibits filamentary structure. We can see from Fig. 2(a) that n_2 has indeed suppressed the catastrophic self-focusing that leads to filamentation. However, this α -induced self-focusing is not completely quenched as noted by the “squeezing” near the center of the current stripe. The twin-lobed far-field profile shown in Fig. 2(b) is evidence of a curved wave front, which is a typical feature of such gain-guided devices.¹⁴ As the injected current is increased to 5 times above threshold, the device remains in the stable region shown in Fig. 1(b). However, the effective index reduction in the self-defocusing layers has increased since it depends on n_2 times the mode intensity. Figures 2(c) and 2(d) display the near- and far-field profiles, respectively, for this case. Notice that n_2 has completely compensated for any α -induced self-focusing as evident by the flatness of the lat-

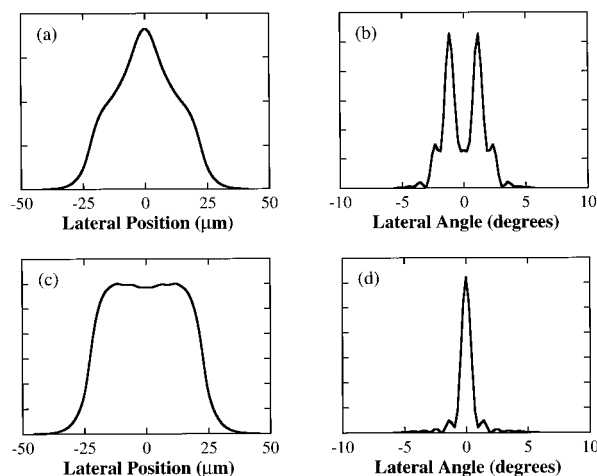


FIG. 2. Normalized near field (left column) and far field (right column) profiles for a $50\text{-}\mu\text{m}$ -stripe-width laser operating 2.5 times above threshold (upper row) and 5 times above threshold (lower row). In both cases $\alpha=1$ and $(1-\Gamma)n_2=-5\times 10^{-12}\ \text{cm}^2/\text{W}$.

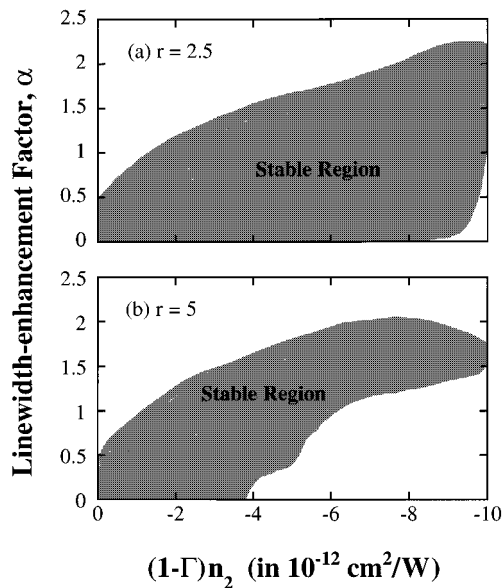


FIG. 3. Same as in Fig. 1 except the stripe width has been changed to $100 \mu\text{m}$.

eral mode profile over the width of the current stripe. Another key point is that the far field is single lobed. Thus, n_2 has also removed the astigmatic curvature that is typically found in gain-guided semiconductor lasers. From a practical standpoint, Fig. 2 shows that, as long as the device remains within the stable region of operation, the lateral mode profile can be tailored by adjusting the injection current.

For high output powers, it is desirable to widen the stripe as much as possible. Figure 3 shows the stability regions for a $100 \mu\text{m}$ stripe at $r=2.5$ and 5 . The qualitative behavior is similar to the $50\text{-}\mu\text{m}$ -stripe case except that the stability region is reduced at a given pumping level. This behavior can be understood by noting that the n_2 -induced index change becomes so large at high pumping levels that it introduces its own set of instabilities which become severe for relatively wide stripes.¹³ Correspondingly, we expect this stability region to shrink as the stripe width is increased. From a design perspective, the optimum value of n_2 depends on both the stripe width w and the pumping level for a given value of α .

How can one implement these numerical results for designing a laterally stable device? In recent years, there have been several reports of devices with values of $\alpha < 2$. Using a multiple-quantum-well (MQW) structure with strained active regions, one group was able to produce a laser with a mea-

sured value $\alpha=1$.¹⁵ We propose to use a pair of self-defocusing layers of thickness $\sim 0.1 \mu\text{m}$ sandwiched between the MQW active region and the cladding layers. For example, to achieve a value of $n_2 = -5 \times 10^{-12} \text{ cm}^2/\text{W}$, the band gap of the new layers should be larger than that of the active layers by 29 meV .⁹ This band gap difference is large enough that it should not affect carrier injection into the quantum wells significantly. In fact, a simple calculation for the density of states of such a quantum well¹⁴ shows that the carrier density in the active layers is large enough to sustain lasing. However, note that thermal activation may induce carrier leakage, thereby increasing the device threshold.

In conclusion, the nonlinear phenomenon of self-defocusing occurring inside new epitaxial layers of a broad-area semiconductor laser can play an important role in controlling filamentation. It can be used to stabilize the lateral mode by tailoring the band gap difference between the active and the new self-defocusing layers. We have suggested the design of such a laterally stable broad-area laser by using a strained MQW active region since α values are relatively low for such structures. Although our simulations considered broad-area semiconductor lasers, qualitatively similar behavior is expected to occur for amplifier and MOPA devices.

- ¹A. H. Paxton and G. C. Dente, *J. Appl. Phys.* **70**, 1 (1991).
- ²M. Tamburrini, L. Goldberg, and D. Mehuys, *Appl. Phys. Lett.* **60**, 1292 (1992).
- ³R. J. Lang, D. Mehuys, A. Hardy, K. M. Dzurko, and D. F. Welch, *Appl. Phys. Lett.* **62**, 1209 (1993).
- ⁴H. Adachi, O. Hess, E. Abraham, P. Ru, and J. V. Moloney, *J. Opt. Soc. Am. B* **10**, 658 (1993).
- ⁵R. J. Lang, D. Mehuys, D. F. Welch, and L. Goldberg, *IEEE J. Quantum Electron.* **30**, 685 (1994).
- ⁶O. Hess, S. W. Koch, and J. V. Moloney, *IEEE J. Quantum Electron.* **31**, 35 (1995).
- ⁷L. Goldberg, M. R. Surette, and D. Mehuys, *Appl. Phys. Lett.* **62**, 2304 (1993).
- ⁸D. J. Bossert, J. R. Marciante, and M. W. Wright, *IEEE Photonics Technol. Lett.* **7**, 470 (1995).
- ⁹M. J. LaGasse, K. K. Anderson, C. A. Wang, H. A. Haus, and J. G. Fujimoto, *Appl. Phys. Lett.* **56**, 417 (1990).
- ¹⁰B. S. Wherrett, A. C. Walker, and F. A. P. Tooley, in *Optical Nonlinearities and Instabilities in Semiconductors*, edited by H. Haug (Academic, San Diego, 1988), Chap. 10.
- ¹¹G. P. Agrawal, *J. Appl. Phys.* **56**, 3100 (1984).
- ¹²G. C. Dente and M. L. Tilton, *IEEE J. Quantum Electron.* **20**, 76 (1993).
- ¹³J. R. Marciante and G. P. Agrawal, *IEEE J. Quantum Electron.* **32**, 590 (1996).
- ¹⁴G. P. Agrawal and N. K. Dutta, *Semiconductor Lasers*, 2nd ed. (Van Nostrand Reinhold, New York, 1993).
- ¹⁵F. Kano, T. Yamanaka, N. Yamamoto, H. Mawatari, Y. Tohmori, and Y. Yoshikuni, *IEEE J. Quantum Electron.* **30**, 533 (1994).